

# Synthesis of Mesoporous Cu-Mn-Al<sub>2</sub>O<sub>3</sub> Materials and Their Applications to Preferential Catalytic Oxidation of CO in a Hydrogen-rich Stream

FANG De-ren<sup>1,2</sup>, REN Wan-zhong<sup>2</sup>, LIU Zhong-min<sup>1\*</sup>, XU Xiu-feng<sup>2</sup>,  
ZHANG Hui-min<sup>2</sup> and LIAO Wei-ping<sup>2</sup>

1. Dalian Institute of Chemical Physics, Chinese Academy of Sciences, Dalian 116023, P. R. China;

2. Institute of Applied Catalysis, Yantai University, Yantai 264005, P. R. China

**Abstract** A series of mesoporous Cu-Mn-Al<sub>2</sub>O<sub>3</sub>(CMA) materials was synthesized at moderate temperature and their structures were characterized by XRD, N<sub>2</sub> physical adsorption and TPR techniques. It was found that using metal complex ion[Cu(NH<sub>3</sub>)<sub>4</sub><sup>2+</sup>-Mn(NH<sub>3</sub>)<sub>6</sub><sup>2+</sup>] as raw materials is easier to form good-structure mesoporous Cu-Mn-Al<sub>2</sub>O<sub>3</sub> materials than using its nitrate salt [Cu(NO<sub>3</sub>)<sub>2</sub>-Mn(NO<sub>3</sub>)<sub>2</sub>]. The TPR tests results indicate that CuO and MnO<sub>x</sub> were homogeneously dispersed in the mesoporous materials. Their catalytic application to preferential catalytic oxidation of CO in a hydrogen-rich stream was studied. The activity varies in the order of CMA(1:1, molar ratio) > CMA(1:2) > CMA(2:1) > CMA(CP) > CMA(1:0) ≈ CMA(0:1). The CMA(1:0) and CMA(0:1) have lower activity compared to other samples, implying that there existed coordination effect between Cu-Mn in the samples. The selectivity varied in the order of CMA(0:1) ≥ CMA(1:2) > CMA(1:1) > CMA(2:1) > CMA(1:0) at higher temperature (≥ 120 °C), indicating that increasing the Cu content enhanced the conversion of H<sub>2</sub>. The sample CMA(CP) made by coprecipitation method has a lower CO oxidation activity and selectivity than its counter-parts of mesoporous Cu-Mn-Al<sub>2</sub>O<sub>3</sub> materials[CMA(1:2)], this attributed to the lower surface area of the former and poor interaction of CuO with MnO<sub>x</sub>.

**Keywords** Cu-Mn-Al<sub>2</sub>O<sub>3</sub>; Mesoporous material; Selective CO oxidation; Hydrogen-rich; Catalyst

**Article ID** 1005-9040(2010)-01-105-05

## 1 Introduction

Polymer electrolyte fuel cell(PEFC) systems have received much attention as a compact generator for stationary application and automotive application in vehicles. In this system, hydrogen is used as a fuel, which comes from the partial oxidation of methanol or hydrocarbons, followed by the steam reforming. The problem is that the reformed fuel contains CO at a level of 1%—3% which is adsorbed irreversibly on the Pt electrode of the PEFC at the operating temperature(*ca.* 80 °C), hindering the electrochemical reaction<sup>[1–3]</sup>. Therefore, CO must be removed from the reformed gases to less than  $1 \times 10^{-5}$ — $2 \times 10^{-5}$  before feeding the gas mixture to the Pt electrode. Preferential oxidation(PROX) of CO in the presence of hydrogen is a desirable selection. In the past, a large number of investigations have been carried out on this field, the catalysts using noble metals include supported Pt, Au, Pd, Rh, Ru and so on<sup>[4–7]</sup> as well as

base metals such as Co<sub>3</sub>O<sub>4</sub>, MnO<sub>2</sub>, FeO<sub>x</sub> and CuO-CeO<sub>2</sub><sup>[8,9]</sup>. The supported Pt, Pd, Ru, Rh catalysts have a higher capability for CO oxidation, but have a relatively lower selectivity because their reaction temperature are higher(200 °C). Supported Au catalyst has a higher selectivity and its reaction is moderately(80 °C), while the stability of Au catalyst is a problem for the present. The base metals catalysts have a lower activity for CO oxidation at low temperatures, while their selectivity is lower at higher reaction temperatures. The base metal catalysts were generally prepared by the coprecipitation or impregnation method. Increasing the activity of base metals catalysts at a lower temperature is an interesting task.

Mesoporous material is a kind of material with a regular channel structure and high surface area. Since it was discovered by research group at Mobil Corporation(US) in 1992<sup>[10]</sup>, various synthesis methods have been developed and a great deal of progress has been

\*Corresponding author. E-mail: zml@dicp.ac.cn

Received March 17, 2009; accepted August 26, 2009.

Supported by the Science and Technology Development Project of Shandong Province, China(No.2007GG3WZ03018).

made. Its application in heterogeneous catalysis is a promising field, while the pure silica MCM-41 shows very limited catalytic activities. It is necessary to incorporate metals into the silicate framework to create active sites for catalytic reactions, such as Al, Ti, Cr, V, Sn, Co, Pd, Fe, Ga, Zr, Mn and Cu<sup>[11-18]</sup>. Valange *et al.*<sup>[19]</sup> synthesized a mixed [Cu,Zn,Al] hexagonal and lamellar mesophase. To our knowledge, there have been no reports about the synthesis of Cu-Mn-Al<sub>2</sub>O<sub>3</sub> ternary mesoporous materials. In the present study, a series of Cu-Mn-Al<sub>2</sub>O<sub>3</sub> ternary mesoporous materials was synthesized and their application to preferential catalytic oxidation of CO in a hydrogen-rich stream was studied.

## 2 Experimental

### 2.1 Preparation

The ternary mesoporous materials(Cu-Mn-Al<sub>2</sub>O<sub>3</sub>) were prepared by direct synthesis at moderate temperatures. Lauric acid and polyaluminium chloride were dissolved in distilled water. A mixture of Cu(NH<sub>3</sub>)<sub>4</sub><sup>2+</sup>-Mn(NH<sub>3</sub>)<sub>6</sub><sup>2+</sup> solution was quickly added to the lauric acid-polyaluminium chloride solution with vigorous stirring at 20 °C, followed by the addition of aqueous NaOH(2 mol/L) to adjust the pH value to 9, and continuous stirring was performed for another 30 min. The resultant slurry was transferred into a plastic bottle and aged at 80 °C for 100 h. Then the precipitate was separated by centrifugation and washed with distilled water. The powder product was recovered by filtration and dried at 298 K. The surfactant was removed by calcination at 500 °C in N<sub>2</sub> and then in air for 5 h. The products were designated as CMA(1:0), CMA(2:1), CMA(1:1), CMA(1:2), CMA(0:1), where 1:0, 2:1, 1:1, 1:2 and 0:1 indicate the molar ratio of Cu:Mn in the products, while the (Cu+Mn) content in the products is maintained at 30%(mass fraction).

For comparison, a sample of Cu-Mn-Al<sub>2</sub>O<sub>3</sub> was prepared by coprecipitation method. The aqueous solution of NaOH(2 mol/L) was added to a mixed Cu(NO<sub>3</sub>)<sub>2</sub>-Mn(NO<sub>3</sub>)<sub>2</sub>-Al(NO<sub>3</sub>)<sub>3</sub> solution[its component was equal to that of CMA(1:2)] with vigorous stirring at 20 °C to adjust the pH value to 9, and continuous stirring was performed for another 60 min. Then the precipitate was separated by centrifugation and washed with distilled water, dried at 393 K and calcination was performed at 500 °C in air for 5 h. The sample was designated as CMA(CP).

### 2.2 Characterization

All the as-synthesized and calcined samples of mesoporous Cu-Mn-Al<sub>2</sub>O<sub>3</sub> materials were characterized by powder X-ray diffraction(Shimadzu XRD6100 X-ray powder diffractometer, Cu K $\alpha$  radiation). Nitrogen sorption isotherms were obtained on a Quantachrome NOVA 3000 Instrument. Temperature-programmed reduction(TPR) was performed on a TP5000 multifunction absorber. The catalyst of 50 mg with a particle size of 40—60 mesh was reduced by a mixture of H<sub>2</sub>/N<sub>2</sub>(1:9, volume ratio) in a temperature range of 100—500 °C at a heating rate of 10 °C/min.

### 2.3 Catalytic Testing

The catalytic activities of the catalysts for CO selective oxidation were evaluated in a fixed-bed flow reactor at atmospheric pressure at a space velocity of 20000 h<sup>-1</sup>. The catalyst particle size was 40—60 mesh. The gas mixture with a composition of V(CO):V(O<sub>2</sub>):V(H<sub>2</sub>):V(Ar)=1.0:1.0:80:18 was fed. The products were analyzed by on-line gas chromatography.

Quantitative analysis of H<sub>2</sub>O, CO, CO<sub>2</sub>, and O<sub>2</sub> in the H<sub>2</sub>/Ar matrix was performed by GC(HP5890). Column switching in combination with two-channel detection(thermal conductivity detectors) allowed the separation of CO<sub>2</sub> and H<sub>2</sub>O from the other gas on a polar column(Hayesep Q), followed by the separation of O<sub>2</sub>, Ar, and CO on a 0.5 nm molecular sieve with H<sub>2</sub> as the carrier gas.

The CO conversion, X<sub>co</sub>, was calculated from the CO<sub>2</sub> concentration at the reactor exit. The selectivity was assessed *via* the oxygen mass balance:

$$S = \frac{0.5 \times c_{\text{CO}_2}^{\text{out}}}{c_{\text{CO}_2}^{\text{in}} - c_{\text{O}_2}^{\text{out}}} = \frac{0.5 \times c_{\text{CO}_2}^{\text{out}}}{\Delta c_{\text{O}_2}}$$

## 3 Results and Discussion

### 3.1 Ternary Meso-structured Materials

At first, we prepared the ternary mesoporous materials using Cu(NO<sub>3</sub>)<sub>2</sub>-Mn(NO<sub>3</sub>)<sub>2</sub> instead of Cu(NH<sub>3</sub>)<sub>4</sub><sup>2+</sup>-Mn(NH<sub>3</sub>)<sub>6</sub><sup>2+</sup> as raw materials, and other preparation conditions were completely identical to those demonstrated in previous section. The X-ray diffraction(XRD) patterns of the as-synthesized samples are illustrated in Fig.1. It can be seen from the XRD patterns that all the samples have a peak at 2 $\theta$ =2.2°, but the peak intensities were lower,

indicating that the structures of the samples were not perfect. Ma *et al.*<sup>[20]</sup> studied the formation of manganese oxide mesophases with CTAB as the surfactant under basic conditions. In their work, they have synthesized lamellar manganese oxide mesophases under basic conditions, indicating that under basic conditions the  $Mn^{2+}$  may exist in the form of poly-anion such as  $Mn(OH)_6^{4-}$ . That may explain why the poor-structure was formed in our experiment: the manganese ion (even copper ion may be) did not exist in the form of  $Mn^{2+}$  cation, so it cannot easily be embedded in the framework of mesoporous materials  $Al_2O_3$ , on the contrary it could disturb the polymerization of poly-aluminum to build up a regular structural mesoporous material  $Al_2O_3$ .

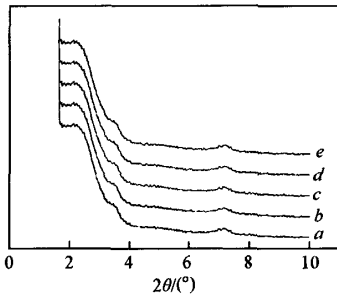


**Fig.1** X-ray diffraction patterns of as-synthesized mesoporous Cu-Mn- $Al_2O_3$  materials with  $Cu(NO_3)_2$ - $Mn(NO_3)_2$  as raw materials

Molar ratio of Cu to Mn: a. 1:0; b. 2:1; c. 1:1; d. 1:2 e. 0:1.

To examine above explanation, we synthesized the ternary mesoporous materials using  $Cu(NH_3)_4^{2+}$ - $Mn(NH_3)_6^{2+}$  as raw materials, X-ray diffraction (XRD) patterns of the as-synthesized and calcined samples are illustrated in Figs.2 and 3, respectively. It is demonstrated from the XRD patterns that both the as-synthesized and calcined samples have the typical XRD patterns of meso-structured materials. What is more, the shapes and positions of XRD peaks of the

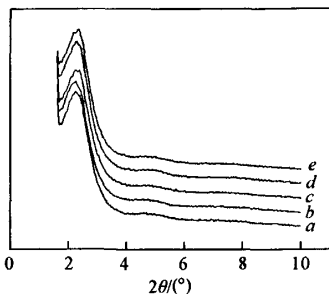


**Fig.2** X-ray diffraction patterns of as-synthesized mesoporous Cu-Mn- $Al_2O_3$  materials with  $Cu(NH_3)_4^{2+}$ - $Mn(NH_3)_6^{2+}$  as raw materials

Molar ratio of Cu to Mn: a. 1:0; b. 2:1; c. 1:1; d. 1:2; e. 0:1.

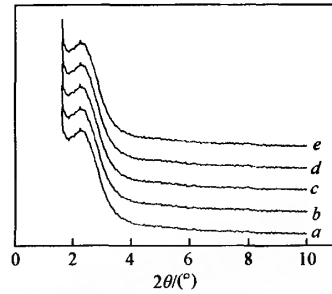


**Fig.3** X-ray diffraction patterns of calcined mesoporous Cu-Mn- $Al_2O_3$  materials with  $Cu(NH_3)_4^{2+}$ - $Mn(NH_3)_6^{2+}$  as raw materials

Molar ratio of Cu to Mn: a. 1:0; b. 2:1; c. 1:1; d. 1:2; e. 0:1.

meso-structured materials are not changed along with the alteration of Cu/Mn molar ratio.

The  $N_2$  adsorption-desorption isotherms of these samples (Fig.4) show that all the curves of CMA(2:1), CMA(1:1) and CMA(1:2) were the isotherms of type IV, e.g. the samples of CMA(2:1), CMA(1:1) and CMA(1:2) have the mesoporous structure, while the curves of CMA(CP) were the isotherms of type III, the sample has macroporous structure. The pore distributions of mesoporous materials and CMA(CP) are illustrated in Fig.5, the pore distribution curves of all the mesoporous materials show a single peak around 20 nm, while that of the sample CMA(CP) shows two

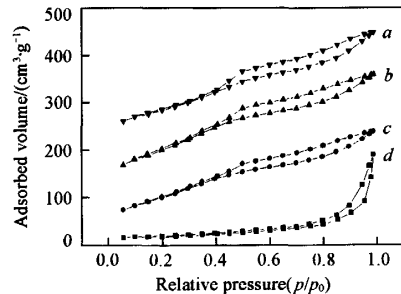


**Fig.4** Nitrogen adsorption and desorption isotherms at 77.3 K

a. CMA(2:1); b. CMA(1:1); c. CMA(1:2); d. CMA(CP).

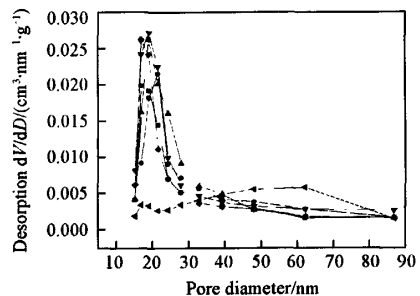


**Fig.5** Pore size distribution curves

■ CMA(1:0); ● CMA(2:1); ▲ CMA(1:1); ▼ CMA(1:2); ◆ CMA(0:1); ◀ CMA(CP).

peaks and very dispersive, its maximum value has shifted to the bigger pore. The surface areas of calcined samples are summarized in Table 1. It is evident that the meso-structured materials have a bigger surface area than the sample prepared by the coprecipitated method.

**Table 1** Structural properties of mesoporous Cu-Mn-Al<sub>2</sub>O<sub>3</sub> materials

| Sample   | BET surface area/<br>(m <sup>2</sup> ·g <sup>-1</sup> ) | Pore volume/<br>(cm <sup>3</sup> ·g <sup>-1</sup> ) | BJH pore size/<br>nm |
|----------|---|---|----------------------|
| CMA(1:0) | 478.6   | 0.4291  | 19.5                 |
| CMA(2:1) | 482.8   | 0.4167  | 19.2                 |
| CMA(1:1) | 503.5   | 0.4354  | 19.7                 |
| CMA(1:2) | 487.1   | 0.4127  | 19.8                 |
| CMA(0:1) | 469.5   | 0.4249  | 19.4                 |
| CMA(CP)  | 103.7   | 0.2427  | 32.9                 |

### 3.2 Reducibility

The TPR profiles(Fig.6) show that the meso-structured materials exhibit a single reduction peak, indicating that CuO and MnO were homogeneously dispersed in the mesoporous materials. This is consistent with the XRD result. On the other hand, sample CMA(CP) exhibits two reduction peaks(Fig.7), implying that in this sample the CuO and MnO existed as partially separated state.

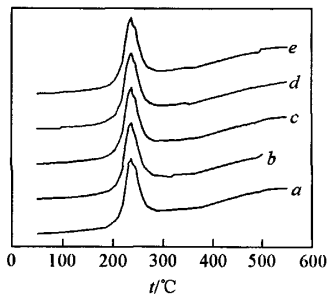


**Fig.6** TPR profiles of calcined mesoporous Cu-Mn-Al<sub>2</sub>O<sub>3</sub> materials

Molar ratio of Cu to Mn: a. 1:0; b. 2:1; c. 1:1; d. 1:2; e. 0:1.

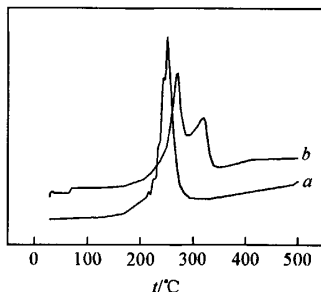
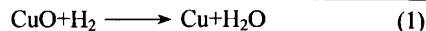


**Fig.7** TPR profiles of calcined mesoporous materials and coprecipitation samples

a. CMA(1:2); b. CMA(CP).

The first reduction peak may be the CuO reduction and Mn<sub>2</sub>O<sub>3</sub> reduction:



while the second reduction peak was the reduction of MnO:



In the case of meso-structured materials CMA, the three reactions occurred at almost the same time, so the TPR profiles show one peak.

The XRD patterns of CMA(2:1), CMA(1:1), CMA(1:2) and CMA(CP) at  $2\theta=10^\circ-80^\circ$ (Fig.8) further verify the supposition. There are no CuO or MnO diffraction peak in the profiles of CMA(2:1), CMA(1:1) or CMA(1:2), while in that of sample CMA(CP), there are three main diffraction peaks of CuO, MnO or CuMn<sub>2</sub>O<sub>4</sub> at  $2\theta=29.95^\circ$ ,  $35.8^\circ$  and  $39.4^\circ$ , respectively.

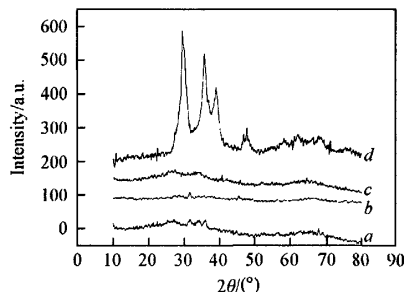


**Fig.8** Wide angle XRD patterns of samples  
a. CMA(2:1); b. CMA(1:1); c. CMA(1:2); d. CMA(CP).

### 3.3 Catalytic Performance

The preferential oxidation of CO was carried out on the six calcined samples with the results illustrated in Figs.9 and 10, respectively. The CO conversion varied with reaction temperature and high temperature favored the reaction up-to 140 °C. After 140 °C, the higher the temperature the lower the CO conversion. The temperature of 140 °C may be the starting temperature of H<sub>2</sub> oxidation. Owing to the content of O<sub>2</sub> in the inlet is constantly, the more O<sub>2</sub> was consumed by H<sub>2</sub>, the fewer O<sub>2</sub> was used for the CO oxidation. The compositions of the samples have a large important effect on the conversion of CO, the activity varied in the order of CMA(1:1)>CMA(1:2)>CMA(2:1)>CMA(CP)>CMA(1:0)≈CMA(0:1). The CMA(1:0) and CMA(0:1) have a lower activity compared to other samples, implying that there exist coordination effect between Cu-Mn in samples<sup>[21]</sup>. By comparison of CMA(1:2) with CMA(CP), one may find the difference of CO conversion is very remarkable.

Reference to the TPR results(Fig.7), we may explain this phenomenon by the coordination effect between Cu-Mn once again, that is to say, in the case of meso-structured Cu-Mn-Al<sub>2</sub>O<sub>3</sub> materials, there exist coordination effect between Cu-Mn, while in the sample of CMA(CP), the interaction of Cu-Mn is small, so the CuO and MnO are reduced separately. Another reason is that the sample CMA(CP) has a lower surface area than its counter-part CMA(1:2).

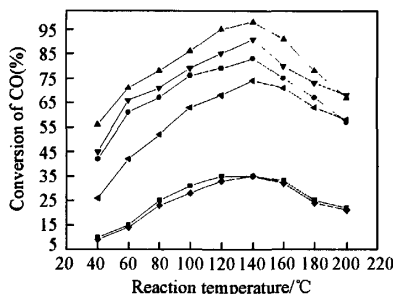


**Fig.9** Evolution of CO conversion with reaction temperature

◆ CMA(0:1); ▼ CMA(1:2); ▲ CMA(1:1);  
● CMA(2:1); ■ CMA(1:0); ◀ CMA(CP).

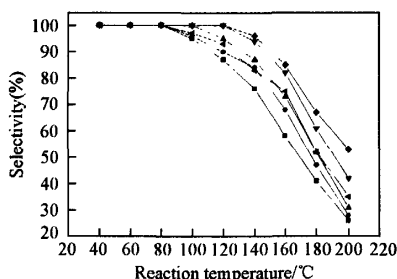


**Fig.10** Evolution of CO oxidation selectivity with reaction temperature

◆ CMA(0:1); ▼ CMA(1:2); ▲ CMA(1:1);  
● CMA(2:1); ■ CMA(1:0); ◀ CMA(CP).

The selectivity varied in the order of CMA(0:1) ≥ CMA(1:2) > CMA(1:1) > CMA(2:1) > CMA(1:0) at a higher temperature (≥ 120 °C), indicating that increasing the Cu content enhanced the conversion of H<sub>2</sub>.

## 4 Conclusions

A series of mesoporous Cu-Mn-Al<sub>2</sub>O<sub>3</sub> materials has been synthesized at moderate temperatures with metal complex ion [Cu(NH<sub>3</sub>)<sub>4</sub><sup>2+</sup>-Mn(NH<sub>3</sub>)<sub>6</sub><sup>2+</sup>] as raw materials. The CuO and MnO<sub>x</sub> were homogeneously dispersed in the mesoporous materials and there existed coordination effect between Cu-Mn in the samples. The catalytic activity and selectivity of mesoporous Cu-Mn-Al<sub>2</sub>O<sub>3</sub> materials is higher than those of the sample made by coprecipitation method for preferential oxidation of CO in a hydrogen-rich stream.

## References

- [1] Luengnaruemitchai A., Osuwan S., Gulari E., *Int. J. Hydrogen Energy*, **2004**, *29*, 429
- [2] Son I. H., Lane A. M., *Catal. Lett.*, **2001**, *76*, 151
- [3] Özbara S., Aksoylu A. E., *Appl. Catal. A*, **2003**, *251*, 75
- [4] Avgouropoulos G., Ioannides T., Papadopoulou C., *et al.*, *Catal. Today*, **2002**, *75*, 157
- [5] Schubert M. M., Plzak V., Garche J., *et al.*, *Catal. Lett.*, **2001**, *76*, 143
- [6] Bethke G. K., Kung H. H., *Appl. Catal. A*, **2000**, *194/195*, 43
- [7] Kahlich M. J., Gasteiger H. A., Behn R. J., *J. Catal.*, **1997**, *171*, 93
- [8] Oh S. H., Sinkevitch R. M., *J. Catal.*, **1993**, *142*, 254
- [9] Sedmak G., Hocevar S., Levec J., *J. Catal.*, **2003**, *213*, 135
- [10] Kresge C. T., Leonowicz M. E., Roth W. J., *et al.*, *Nature*, **1992**, *359*, 10
- [11] Reddy K. M., Moudrakovski I., Sayari A., *Chem. Commun.*, **1994**, (9), 1059
- [12] Abdel-Fattah T. M., Pinnavaia T. J., *Chem. Commun.*, **1996**, (5), 65
- [13] Tuel A., Gontier S., Teissier R., *Chem. Commun.*, **1996**, (5), 51
- [14] Reddy M. K., Wei B., Song C., *Catal. Today*, **1998**, *43*, 61
- [15] Rhee C. H., Lee J. S., *Catal. Today*, **1997**, *38*, 13
- [16] Kosslick H., Lischke G., Landmesser H., *et al.*, *J. Catal.*, **1998**, *176*, 102
- [17] Yonemitsu M., Tanaka Y., Iwamoto M., *J. Catal.*, **1998**, *178*, 207
- [18] Guo X. F., Lai M., Kong Y., *et al.*, *Langmuir*, **2004**, *20*, 2879
- [19] Valange S., Gabeliea Z., *Stud. Surf. Sci. & Catal.*, **1998**, *117*, 952
- [20] Sun X. D., Ma C. L., Wang Y. D., *et al.*, *Mater. Lett.*, **2002**, *54*, 244
- [21] Hutchings G. J., Miraei A. A., Joyner R. W., *et al.*, *Appl. Catal. A*, **1998**, *166*, 143

# Synthesis of Mesoporous Cu-Mn-Al<sub>2</sub>O<sub>3</sub> Materials and Their Applications to Preferential Catalytic Oxidation of CO in a Hydrogen-rich Stream

作者: [FANG De-ren](#), [REN Wan-zhong](#), [LIU Zhong-min](#), [XU Xiu-feng](#), [ZHANG Hui-min](#),  
[LIAO Wei-ping](#)

作者单位: [FANG De-ren](#)(Dalian Institute of Chemical Physics, Chinese Academy of Sciences, Dalian 116023, P.R.China; Institute of Applied Catalysis, Yantai University, Yantai 264005, P.R.China), [REN Wan-zhong](#), [XU Xiu-feng](#), [ZHANG Hui-min](#), [LIAO Wei-ping](#)(Institute of Applied Catalysis, Yantai University, Yantai 264005, P.R.China), [LIU Zhong-min](#)(Dalian Institute of Chemical Physics, Chinese Academy of Sciences, Dalian 116023, P.R.China)

刊名: [高等学校化学研究 \(英文版\)](#) 

英文刊名: [CHEMICAL RESEARCH IN CHINESE UNIVERSITIES](#)

年, 卷(期): 2010, 26(1)

被引用次数: 0次

## 参考文献(21条)

1. [Luengnaruemitchai A. Osuvvan S. Gulari E](#) [查看详情](#) 2004
2. [Son I. H. Lane A M](#) [查看详情](#) 2001
3. [Ozhara S. Aksoylu A E](#) [查看详情](#) 2003
4. [Avgouropoulos G. Ioannides T. Papadopoulou C](#) [查看详情](#) 2002
5. [Schubert M. M. Plzak V. Garche J](#) [查看详情](#) 2001
6. [Bethke G. K. Kung H H](#) [查看详情](#) 2000
7. [Kahlich M. J. Gasteiger H A. Behn R J](#) [查看详情](#) 1997
8. [Oh S. H. Sinkevitch R M](#) [查看详情](#) 1993
9. [Sedmak G. Hocevar S. Levee J](#) [查看详情](#) 2003
10. [Kresge C. T. Leonowicz M E. Roth W J](#) [查看详情](#) 1992
11. [Reddy K. M. Moudrakovski I. Sayari A](#) [查看详情](#) 1994(9)
12. [Abdel-Fattah T. M. Pinnavaia T J](#) [查看详情](#) 1996(5)
13. [Tuel A. Gontier S. Teissier R](#) [查看详情](#) 1996(5)
14. [Reddy M. K. Wei B. Song C](#) [查看详情](#) 1998
15. [Rhee C. H. Lee J S](#) [查看详情](#) 1997
16. [Kosslick H. Lischke G. Landmesser H](#) [查看详情](#) 1998
17. [Yonemitsu M. Tanaka Y. Iwamoto M](#) [查看详情](#) 1998
18. [Guo X. E. Lai M. Kong Y](#) [查看详情](#) 2004
19. [Valange S. GabelieaZ](#) [查看详情](#) 1998
20. [Sun X. D. Ma C L. Wang Y D](#) [查看详情](#) 2002
21. [Hutchings G. J. Miraei A A. Joyner R W](#) [查看详情](#) 1998